UCLA
COMPUTATIONAL AND APPLIED MATHEMATICS

# A Finite Vortex Street Model

Christopher R. Anderson

January 1993

CAM Report 93-01

Department of Mathematics
University of California, Los Angeles
Los Angeles, CA. 90024-1555

# A FINITE VORTEX STREET MODEL

CHRISTOPHER R. ANDERSON*

**Abstract.** In this paper we describe a set of equations (based on the incompressible two dimensional Euler equations) whose solutions provide a vortex street of finite length. We describe a second order accurate numerical procedure for solving these equations. In our description we introduce a technique for incorporating point sources within a vortex blob method and a technique for removing vorticity "gracefully" from the computation. The solution of the equations is easily and quickly generated, thus providing a computational useful simulation of a finite wake.

**1. Introduction.** This work was motivated by the desire to have a numerical simulation of a vortex street, or wake, which forms behind a bluff body as it is moved through a fluid. We did not want to assume that the flow was periodic, and so the common method for generating a vortex street could not be used. (One just perturbs a two dimensional shear layer composed of oppositely signed vorticity) Also, for simplicity, and because we were only interested in wake phenomenon, we did not want to use a full simulation of the Navier-Stokes equations (or other model equations) for flow past a blunt body.

The simulation that we present is based on using a vortex blob method to solve the incompressible Euler equations in which there are point sources of vorticity. The equations will be described in section 1, but one can understand the idea without the equations. Given a uniform background velocity (say $\vec{v} = (1, 0)$) we use two point sources of vorticity that contribute oppositely signed vorticity. When implemented numerically, the introduction of vorticity is accomplished by introducing vortex blobs (or point vortices if you like) at the source locations at each time-step. After vortices are introduced into the flow they move according to the equations derived from the inviscid Euler equations. With an appropriate choice of numerical parameters the motion that the vortices exhibit has many features in common with a vortex street. To limit the number of vortices that participate in the simulation, we remove vortices that have existed for a prescribed length of time. See Figure 1 for a schematic of the simulation.

The primary purpose of this paper is to describe the two aspects of the simulation that have to be treated carefully - how one creates vortices and how one removes vortices. Both aspects have to be done carefully to preserve time accuracy in the simulation. In the first section we give the relevant equations, in the second section we describe a numerical procedure to solve these equations, and in the third section we give computational results.

**2. The Equations.** A vortex blob method for solving the vorticity form of the incompressible Euler equations in two dimensions consists of identifying a collection of N vortex blobs and evolving their positions and their strengths. (From the positions and strengths of the blobs we can obtain a vorticity distribution that gives an approximate solution of Euler's equations.) If the $i$th vortex blob is at the point $\vec{x}_i(t) = (x_i(t), y_i(t))$ and has strength $\sigma_i(t)$, then these quantities evolve according to the ordinary differential equations

* Department of Mathematics, UCLA, Los Angeles, California, 90024
Research Supported by Air Force Office of Scientific Research Contract #F49620-92-J-0279

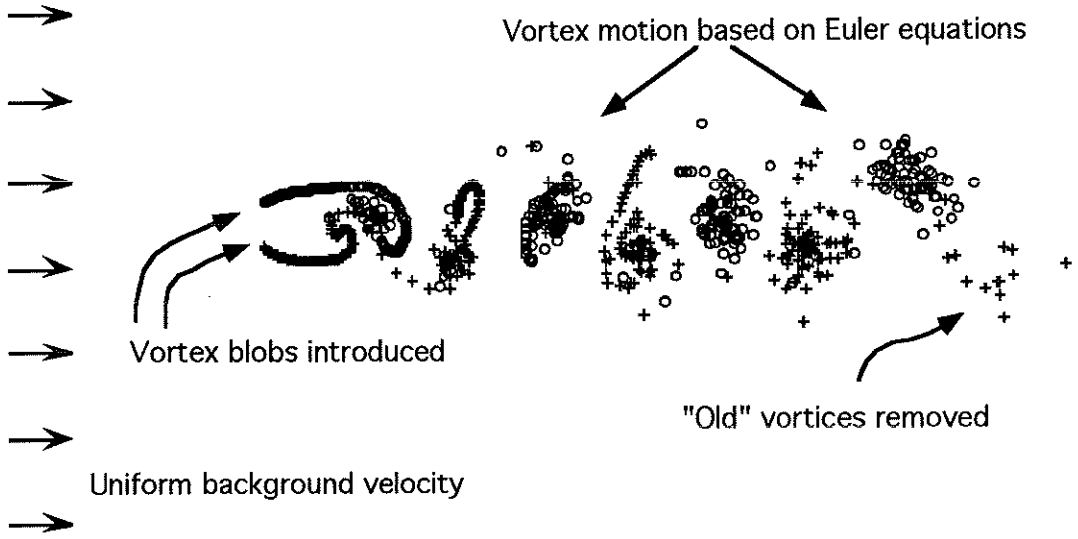


FIG. 1. *A schematic of a vortex simulation of a finite vortex street.*

$$\frac{d\vec{x}_i}{dt} = \vec{u}_\delta(\vec{x}_i(t), t) + \vec{v}(\vec{x}_i(t)) \qquad \vec{x}_i(0) = \vec{x}_i^0 \tag{1}$$

$$\frac{d\sigma_i}{dt} = f_i(t) \qquad \sigma_i(0) = \sigma_i^0 \tag{2}$$

where $\vec{u}_\delta$ is the velocity field induced by the collection of vortex blobs ;

$$\vec{u}_\delta(\vec{x}, t) = \sum_{i=1}^{N} \vec{K}_\delta(\vec{x} - \vec{x}_i)\, \sigma_i(t). \tag{3}$$

Here $\vec{K}_\delta$ is a mollified version of the Biot-Savart kernel

$$\vec{K}(\vec{x} - \vec{x}') = \frac{(-(y - y'), (x - x'))}{2\pi ||\vec{x} - \vec{x}'||}$$

and $\delta$ is the smoothing parameter. The specific formula we use for $\vec{K}_\delta$ will be given in section 2. The velocity $\vec{v}(\vec{x})$ corresponds to a potential flow - i.e. a time independent solution of the Euler equations with no vorticity. In our simulation, this will be a uniform flow in the $x$ direction, i.e. $\vec{v}(\vec{x}) = (1, 0)$.

For a pure initial value problem associated with the Euler equations the function $f_i(t)$ in (2) is identically zero, and the value of $\sigma_i$ for each vortex is just its initial value. In our simulation we are interested in a solution for the incompressible Euler equations that has a time-dependent source, and thus we will use an $f_i(t)$ that accounts for this. We also will use $f_i(t)$ to force the vortex strengths to decay after a certain period of time. (We then remove the vortices whose strengths have decayed to zero.) For a more thorough discussion of the derivation of the equations for vortex methods and a convergence analysis one can consult [2] as well as the references contained therein.

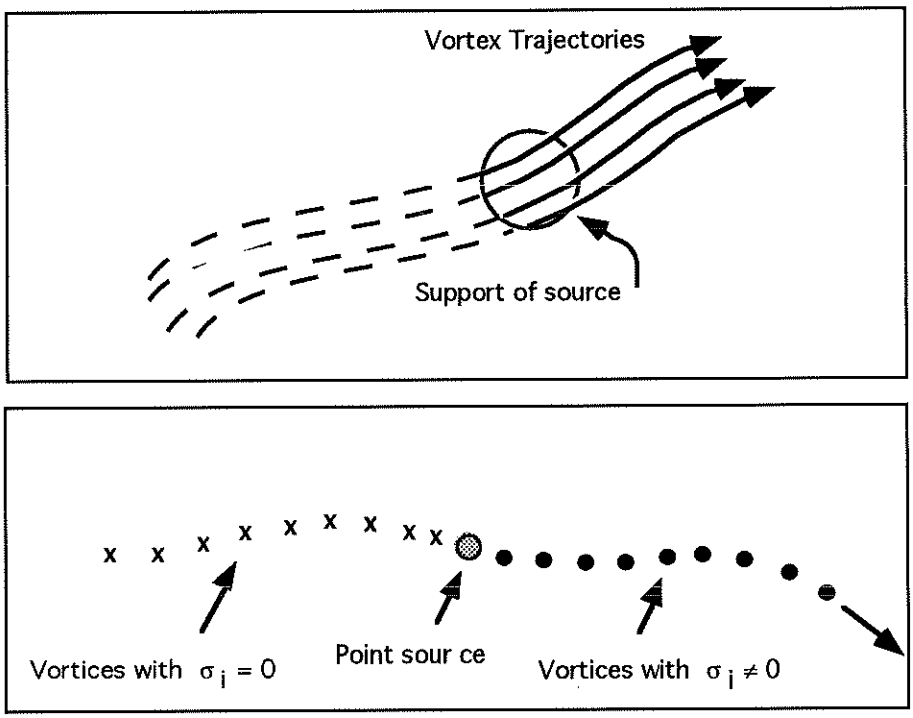


FIG. 2. *(a) Vortex trajectories passing through the support of the vorticity source function and accumulating strength. (b) Vortices passing through a point source and accumulating strength.*

To motivate our treatment of the source term, we consider the form that $f_i(t)$ takes when the source is not a point source, but one that is non-zero over a region of a finite size. If $s(\vec{x}, t)$ is the source function, then by considering the Euler equations written in Lagrangian form, $f_i(t) = s(\vec{x}_i(t), t)$ and so we have the equation

$$\frac{\mathrm{d}\sigma_i}{\mathrm{d}t} = s(\vec{x}_i(t), t). \tag{4}$$

Thus, as a vortex passes through the support of the source (where the source is non-zero), its strength accumulates corresponding to the value of the source at the vortex's instantaneous location. A diagram of the situation is presented in Figure 2(a). For this figure we have assumed that the support of the source is contained inside a disk of finite size. The change in the strength of vortices is indicated by their trajectories changing from dashed to solid lines. To capture accurately the effect of a source one must have many vortices pass through the source. One mechanism for ensuring this is to introduce vortices with zero strength just upstream of the source and have them flow through the source region (for example see [3]).

The treatment of a point source or collection of point sources is analogous to the treatment of a spatially distributed source. If the position of a point source is $\vec{x}_{source}$ then $f_i(t)$ is given by

$$f_i(t) = \left\{ \begin{array}{rl} s(\vec{x}_{source}, t) & \text{if} \quad \vec{x}_i = \vec{x}_{source} \\ \\ 0 & \text{if} \quad \vec{x}_i \neq \vec{x}_{source} \end{array} \right\}$$

Figure 2(b) illustrates the accumulation of vortex strength by vortices that pass through the source. While we only show a discrete set of vortices in this figure, the correct situation is one in which a continuum of vorticity passes through the source. The result of such a source is the generation of a vortex sheet.

As one can infer from the above discussion, the mechanism by which vortices are "created" consists of vortices of zero strength (or just Lagrangian particles) passing through a source and accumulating strength. Since one does not need to track vortices of zero strength (they do not contribute to the velocity field and therefore do not influence the fluid motion), one need only track vortices after the time that they first encounter a source. In a calculation, the identification of a vortex that is encountering a source consists of adding that vortex to an existing collection of vortices. We will refer to this identification as the "introduction" or "creation" of vorticity by the source. However, precisely speaking, we are not creating a vortex, we are merely identifying it.

In the simulation we would like to have a finite number of vortices to keep the computational cost down. To do this we modify $f_i(t)$ to cause the strength of any vortex that is sufficiently "old" to diminish, and then remove any vortex whose strength has become sufficiently small. Our particular construction of an $f_i(t)$ for this purpose this does not correspond to a term in the Euler equations, and it is just a mechanism by which we remove vorticity. In our simulation every vortex that we introduce will have a time $t_i^*$ associated with it that indicates the time at which the vortex was generated. (Or, with regard to the discussion above, $t_i^*$ is the time that the vortex first passes over a source location.) For the $i$th vortex and $t > t_i^*$ we use

$$f_i(t) = p(t - t_i^*)\,\sigma_i(t) \tag{5}$$

where a single function $p(s)$ is chosen to be zero if $s < t_{fade}$ and chosen to have non-zero values for $s \geq t_{fade}$. Here $t_{fade}$ is the age at which a vortex's strength starts to diminish. The values of $p(s)$ are chosen to ensure that the strength $\sigma_i(t)$ tends to zero for $s \geq t_{fade}$.

If we incorporate the above specification of $f_i(t)$ in (2), then the equation for the change in the strength of vorticity becomes

$$\frac{\mathrm{d}\sigma_i}{\mathrm{d}t} = \begin{cases} \left\{ \begin{array}{ll} s(\vec{x}_{source},\, t) & \text{if} \quad \vec{x}_i = \vec{x}_{source} \\ 0 & \text{if} \quad \vec{x}_i \neq \vec{x}_{source} \end{array} \right\} & \text{for} \quad t - t_i^* < t_{fade} \\ p(t - t^*)\,\sigma_i(t) & \text{for} \quad t - t_i^* \geq t_{fade} \end{cases} \tag{6}$$

where $\vec{x}_{source}$ is a source location and $t_i^*$ is the time at which the $i$th trajectory first passes though a source location.

**3. The Numerical Method.** In this section we describe the numerical method for solving the equations (1) and (6) as well as give formulas for our choice of $\vec{K}_\delta$ and the function $p(s)$ used to enforce vortex decay.

We will describe two numerical procedures. Both of the numerical procedures are based on the method of fractional steps. Essentially we solve for the change in the vortex strength for one fractional step and for the movement of the vortices during the other fractional step. If one alternates these steps the resulting method is first order

accurate in time. To get a second order accurate method we use the idea of Strang splitting [5]. The fractional step method is particularly attractive for this problem because it decouples the change in vortex strength from the vortex movement. This decoupling proved to be extremely useful in the derivation of a second order method. If one doesn't decouple these two components, then one gets complicated procedures because the vortex creation (necessary due to the sources) is intertwined with the vortex movement.

The first fractional step consists of solving (6) for a timestep $\Delta t$. At the beginning of this step we introduce new vortices with zero strength at the point source locations. (One could think of this introduction as identifying vortices that have travelled from upstream and just landed at the source points.) For each of the newly introduced vortices, the function $f_i$ will be non-zero, and thus the strength of the vortices will be non-zero at the end of the fractional step. With each new vortex we associate a time of introduction $t_i^*$ with it. The differential equation (6) that governs the strength of the new vortices is particularly simple — the right hand side is the prescribed function of time $s(\vec{x}_{source}, t)$. Thus, to solve the differential equation one just integrates this source function over a length of time $\Delta t$. We used the midpoint rule - so that for a new vortex at a source point $\vec{x}_{source}$,

$$\sigma_i^{n+1} = \sigma_i^n + \Delta t\, s(\vec{x}_{source}, t^n + \frac{\Delta t}{2}). \tag{7}$$

For those vortices whose age, $t - t_i^*$, is less than $t_{fade}$, the function $f_i(t)$ is identically zero, and so their strengths are unchanged during this fractional step.

For the vortices whose age is greater than $t_{fade}$ their strength must be modified by equation (6). For such vortices equation (6) can be solved exactly. Since $p(s) = 0$ for $s < t_{fade}$, for the $i$th particle for which $t - t_i^* > t_{fade}$,

$$\sigma_i(t) = \tilde{\sigma}_i \, e^{\int_{t_{fade}}^{t-t_i^*} p(u)du}. \tag{8}$$

Here $\tilde{\sigma}_i = \sigma_i(t_{fade} + t_i^*)$ is the value of the strength just before the decay process begins.

It was our desire to choose $p(s)$ so that the vortices would have zero strength after some finite time $\delta t_{fade}$. To do this we picked $p$ so that the exponential factor in (8) simplified a polynomial that had the value one at $t = t_{fade} + t_i^*$ and decayed to zero at $t = t_{fade} + t_i^* + \delta t_{fade}$. We used

$$p(u) = \left(\frac{1}{\delta t_{fade}}\right) \frac{\left[ -30\,(\frac{u-t_{fade}}{\delta t_{fade}})^4 + 60\,(\frac{u-t_{fade}}{\delta t_{fade}})^3 - 30\,(\frac{u-t_{fade}}{\delta t_{fade}})^2 \right]}{1 - \left[ 6\,(\frac{u-t_{fade}}{\delta t_{fade}})^5 - 15\,(\frac{u-t_{fade}}{\delta t_{fade}})^4 + 10\,(\frac{u-t_{fade}}{\delta t_{fade}})^3 \right]} \tag{9}$$

and so

$$e^{\int_{t_{fade}}^{t-t_i^*} p(u)du} = 1 - \left[ 6\,(\frac{s-t_{fade}}{\delta t_{fade}})^5 - 15\,(\frac{s-t_{fade}}{\delta t_{fade}})^4 + 10\,(\frac{s-t_{fade}}{\delta t_{fade}})^3 \right] \tag{10}$$

where $s = t - t_i^*$. This latter function is twice continuously differentiable for $s \in [t_{fade}, t_{fade} + \delta t_{fade}]$.

To update the strength of the vortices that should decay, we evaluated the exact solution (8). When a vortex had zero strength (i.e. its age was greater than $t_{fade} + \delta t_{fade}$) then the vortex was deleted from the computation. A benefit of using the exact solution is that the time-step difficulties associated with solving (6) numerically are avoided. Numerical problems would arise because of the singular nature of $p(s)$. ($p(s)$ must be singular so that the vortices decay to zero in finite time.)

The second fractional step consisted of moving the vortices using equation (1) with their strengths fixed. The velocity field $\vec{u}_\delta(\vec{x})$ is evaluated explicitly using the formula (3). The formula we used for $\vec{K}_\delta$ was that obtained by mollifying the kernel $\vec{K}$ with the function

$$\psi_\delta(\vec{x}) = \begin{cases} \frac{1}{4\pi\delta^2}\left(1 - (\frac{|\vec{x}|}{\delta})^2\right)^3 & |\vec{x}| \le \delta \\ 0 & |\vec{x}| > \delta \end{cases} \tag{11}$$

(or equivalently, $\psi_\delta(\vec{x})$ is the form of our vortex blobs). The resulting expression for $\vec{K}_\delta$ is

$$\vec{K}_\delta(\vec{x} - \vec{x}') =$$

$$\begin{cases} \frac{1}{2\pi\delta^2}(-(y-y')\,,\, x-x')\left(4 - 6\left(\frac{r}{\delta}\right)^2 + 4\left(\frac{r}{\delta}\right)^4 - \left(\frac{r}{\delta}\right)^6\right) & r \le \delta \\ \frac{1}{2\pi}\left(\frac{-(y-y')}{r^2}\,,\, \frac{x-x'}{r^2}\right) & r > \delta \end{cases} \tag{12}$$

Here $r = \sqrt{(x-x')^2 + (y-y')^2}$.

A first order numerical method consists of solving the vortex strength equation (6) for $\Delta t$ followed by a solution to (1) for $\Delta t$ . The combination of these two fractional steps is one timestep of the whole solution. In the first fractional step new vortices are created at point source locations. To carry out the second step one can use any standard numerical solution procedure — we used forward Euler.

A second order numerical method can be obtained by using Strang splitting [5]. The method consists of solving the vortex strength equation for $\frac{\Delta t}{2}$ (with vortex creation), solving the vortex transport equation (1) for $\Delta t$ and then solving solving the vortex strength equation for $\frac{\Delta t}{2}$ (again with vortex creation). These three substeps combine to yield one timestep in the solution of the whole system. For the solution of (1) we used a second order Runge-Kutta method (Huen's method). Also, when carrying out the solution of the vortex strength equation in the third component of the calculation, the time at which the integration of the source term begins is $t^n + \frac{\Delta t}{2}$, not $t^n$. By doing a Taylor series analysis one finds that this splitting strategy is formally second order accurate. The computational results presented in the next section also demonstrate the second order accuracy.

Since there are two steps of the vortex strength equation in the second order method per timestep, it appears that the second order method will introduce twice as many vortices as the first order method. This can be avoided. In the second order method the vortices don't move between the end of a timestep and the beginning of a new timestep, so, at the beginning of the first substep one can use the vortices that are already at the source points from the previous substep. Therefore, similar to the first order method, one introduces just one new vortex per source point per timestep.

**4. Numerical Results.** The numerical results that we present show the accuracy of the numerical procedures and that with an appropriate set of numerical parameters the solutions to equations (1) and (6) have the qualitative features of a finite vortex street. In all our computations there was a prescribed background flow velocity $\vec{v}(\vec{x}) = (1, 0)$ and two point sources of vorticity located a unit distance apart on the y-axis, at $(0, \frac{1}{2})$ and $(0, -\frac{1}{2})$. The size of the smoothing parameter $\delta$ for the vortex blobs was .5.

In our computations we wanted to have a source that was a smooth function of time so we used

$$(13) s(t) = \begin{cases} \alpha \left[ \; 6\,(\frac{t}{t_{startup}})^5 \; - \; 15\,(\frac{t}{t_{startup}})^4 \; + \; 10\,(\frac{t}{t_{startup}})^3 \; \right] & t \leq t_{startup} \\ \\ \alpha & t > t_{startup}. \end{cases}$$

The polynomial function occurring in this expression is one that provides a smooth transition from zero to one over a time interval of length $t_{startup}$. The value of $t_{startup}$ was 0.4 and the strength of the source $\alpha$ was -4.0 for the point source at $(0, \frac{1}{2})$ and 4.0 for the point source at $(0, -\frac{1}{2})$. To make the solution non-symmetric (and therefore more interesting) we included an initial vortex of strength 1 located at the point (0,2). For the decay parameters we used, $t_{fade} = 1$, and $\delta t_{fade} = 5$. The accuracy of the solution was assessed by considering the behavior of the vertical velocity at the origin, i.e. (3) evaluated at (0,0). In Figure 3(a) and Figure 3(b) we show the vertical velocity obtained using both the first order and the second order method for $t \in [0, 2]$. These results were computed with timesteps $\Delta t = .1$, .05, and .025. With a timestep of $\Delta t = .05$ we find that the second order method has captured the solution over the interval $t \in [0, 2]$, while the first order method has not. In fact, the timestep that must be used with the first order method to obtain solutions close to those obtained with the second order method was on the order of $\Delta t = .0015$.

The rate of convergence for each method was estimated using Aitken extrapolation [1]. At a fixed time, the values of the vertical velocity were computed using three different timesteps, say $\gamma_{.1}$, $\gamma_{.05}$, and $\gamma_{.025}$. The estimate of the rate of convergence is given by

$$\rho = \frac{\gamma_{.05} - \gamma_{.1}}{\gamma_{.025} - \gamma_{.05}}$$

The rates of convergence at times over the interval $[0, 2]$ are presented in Figure 3(c). For short times, the estimated rate of convergence for both methods coincides with the expected rate of convergence. The rate of convergence fluctuates after time t=1.0, but this appears to be caused by the fact that the stepsizes used are large and we are not in the "asymptotic" regime which is necessary for the extrapolation estimate to be accurate. If one chooses smaller stepsizes, then one can verify the order of accuracy for longer periods of time.

The next set of results, presented in figures 4(a)-4(d), show that the solutions of these equations exhibit the behavior of a finite vortex street. In these simulations the strength $\alpha$ in (13) was -0.85 for the point source at $(0, \frac{1}{2})$ and 0.85 for the point source at $(0, -\frac{1}{2})$. Also, $t_{startup} = .2$, $t_{fade} = 15.0$ and $\delta t_{tfade} = 5.0$. In these calculations there was an initial vortex of strength 1 located at the point $(0, 2)$. This initial vortex was included as a non-symmetric perturbation. Without such a vortex the solution remains symmetric and does not develop into a vortex street pattern.

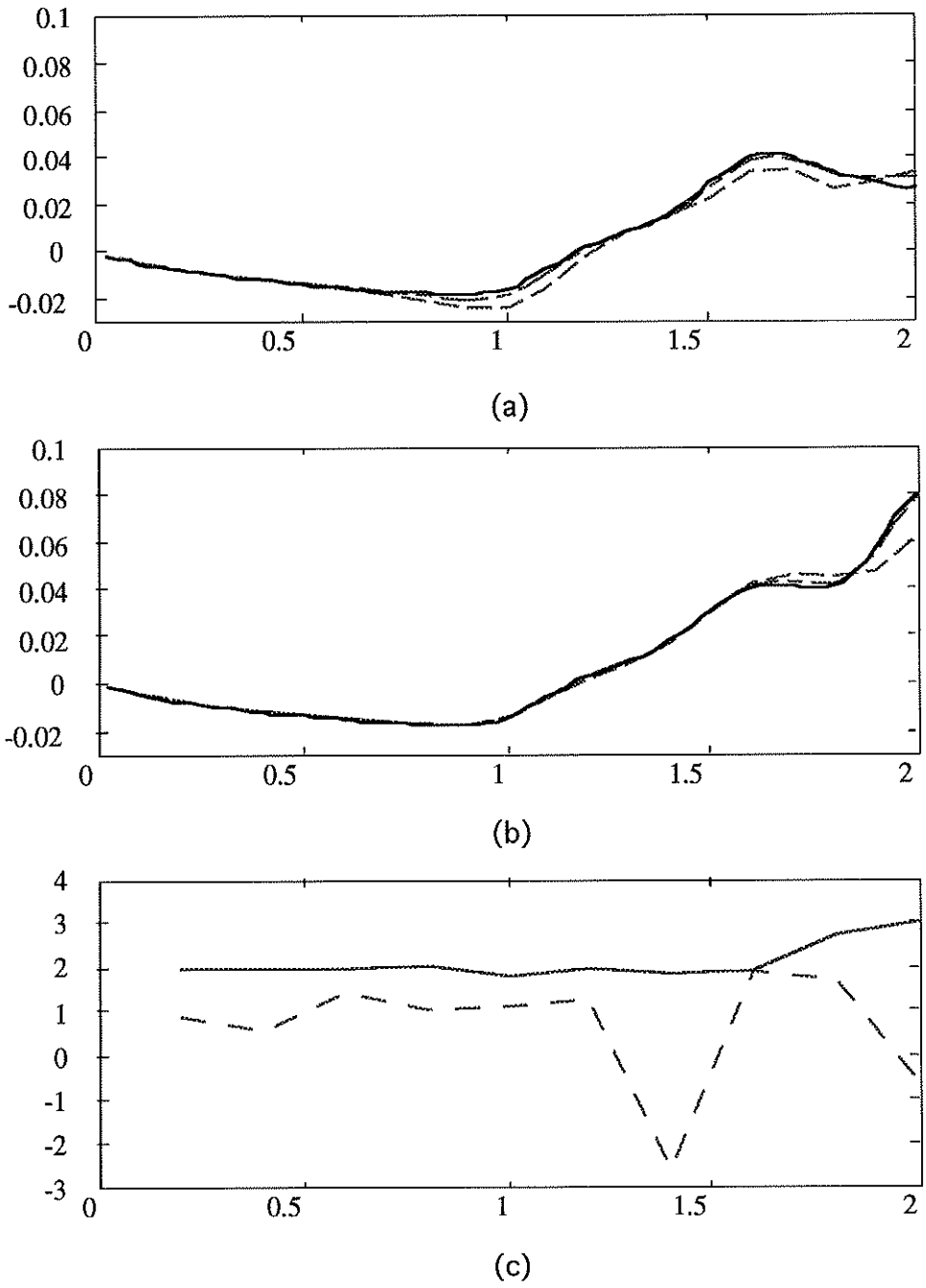


FIG. 3. *(a) Vertical velocity at the origin verses time for the first order method. $\Delta t = .1$ : short dash line, $\Delta t = .05$ : short/long dash line, and $\Delta t = .025$ : solid line. (b) Vertical velocity at the origin verses time for the second order method. $\Delta t = .1$ : short dash line, $\Delta t = .05$ : short/long dash line, and $\Delta t = .025$ : solid line.. (c) Extrapolated rates of convergence. First order method : short dash line and second order method :solid line.*

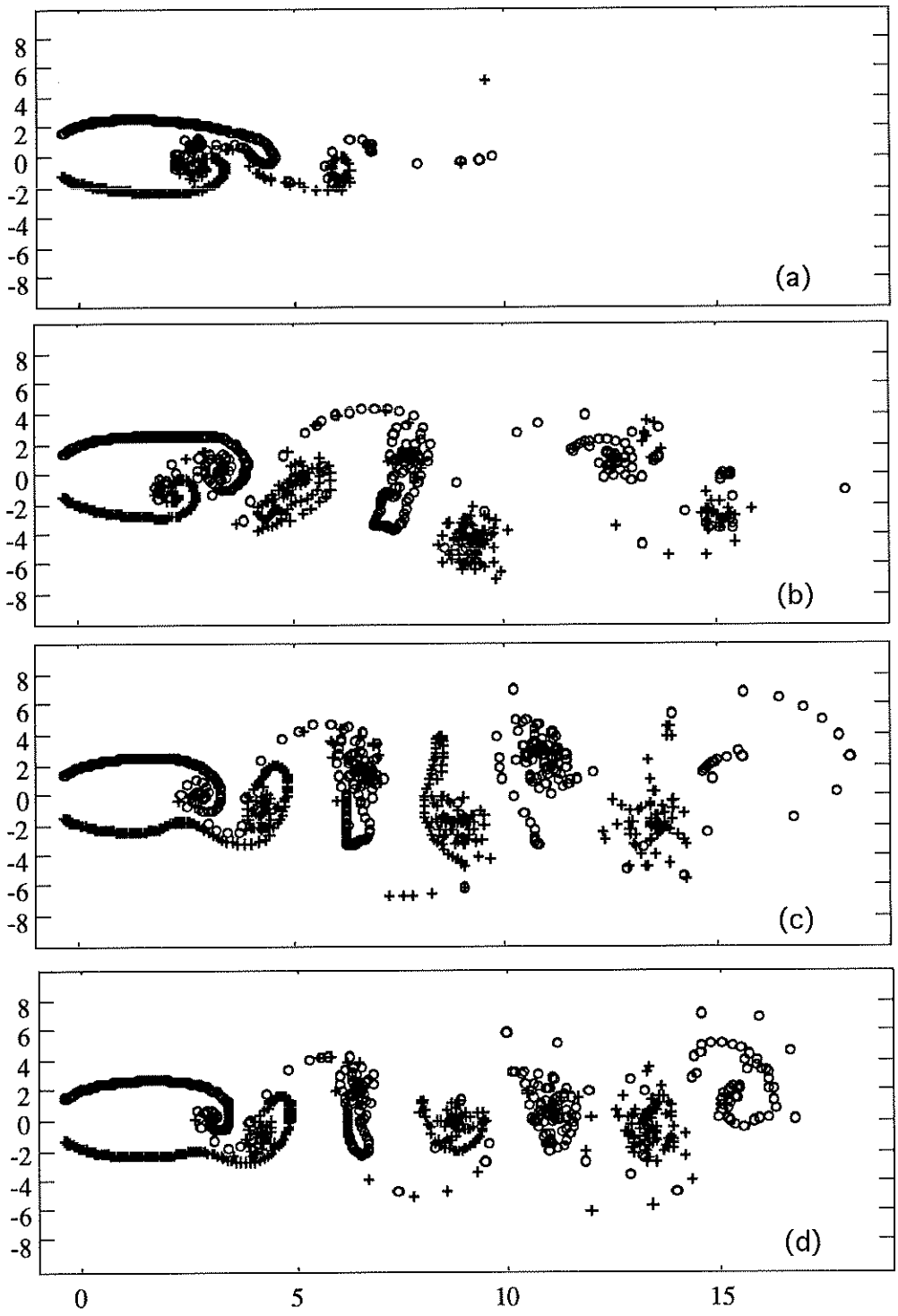


FIG. 4. *Vortex locations at different times. Vortices with negative strength are represented by circles and vortices with positive strength are represented by plus signs. (a)* $t = 10.0$, *(b)* $t = 20.0$, *(c)* $t = 30.0$ *and (d)* $t = 40.0$.

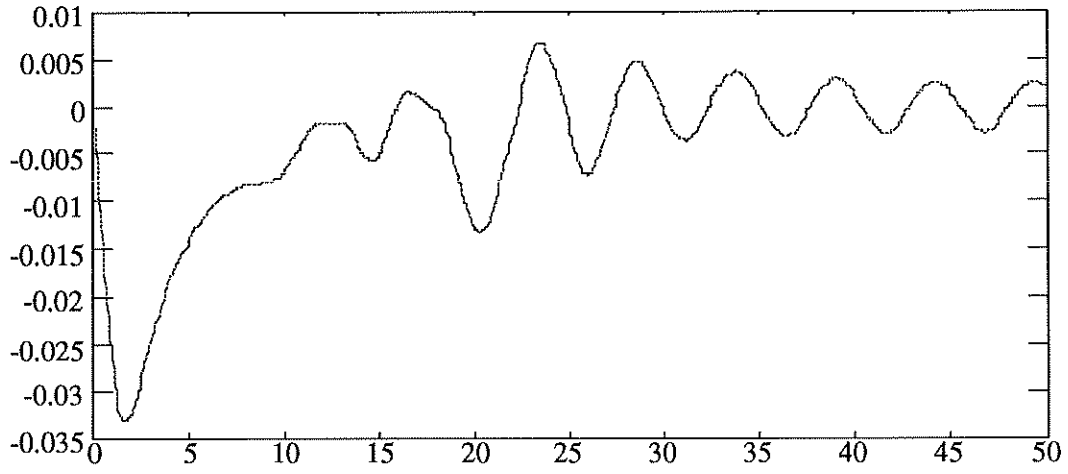


FIG. 5. *Vertical velocity at the origin as a function of time for the computation whose vortex positions are given in Figure 4.*

In the figures the vortices with positive strength are represented by "+" signs and those with negative strength are indicated by the symbol "o". As one can see, a pattern of large vortical structures with alternating signed vorticity forms behind the source. The solution pattern shown in figure 4(d) is very stable. In figure 5 we show the vertical velocity at the origin as a function of time. The periodic nature of the flow is clearly in evidence.

While the vortex street pattern that is shown in figure 4 occurs over a wide range of parameter choices, the parameters do have an effect on the solution. If one increases the value of $t_{fade}$, then a longer vortex street forms. If the magnitude of the vorticity that is introduced per unit time is changed ($\alpha$ in (13)) then the distance downstream at which the large vortices form into a vortex street is changed. For values of $\alpha$ above .85, the vortex street forms closer to the source points than that shown in figure 4(d), and for values of $\alpha$ less than this, the vortex street begins to form further downstream. If the value of $\alpha$ is sufficiently large, then the vortices that form translate in the negative x-direction and eventually pass the source location. In this case the solution is not particularly well behaved. If the magnitude of the introduced vorticity is much smaller than .85, then the vortices do not roll up appreciably before they are eliminated from the computation and so no vortex street forms.

**5. Conclusion.** The main contribution of this paper is the demonstration that there are solutions of the incompressible Euler equations with point sources of vorticity that exhibit vortex street structure. If one uses a Lagrangian method to solve the equations, such as we have done here, then one can truncate the solutions by discarding "old" vorticity. In this way one can create a finite vortex street. With the numerical method described here the solutions can be obtained with a modest computational cost, and so the solutions can conveniently provide simulations of a wake for other analytical or numerical investigations. Also, the numerical techniques for vorticity elimination and inclusion of points sources presented here may be useful in other vortex method simulations - for example those in which a bluff body is included (e.g. [4]).

## REFERENCES


[1] K. E. ATKINSON, *An Introduction to Numerical Analysis*, Wiley, 1978.

[2] C.ANDERSON AND C.GREENGARD, *On vortex methods*, SIAM J. Numer. Anal., 22 (1985), pp. 413–440.

[3] G. COTTET, *Particle-grid domain decomposition methods for the navier-stokes equations in exterior domains*, in Vortex Dynamics and Vortex Methods, C. R. Anderson and C. Greengard, eds., vol. 28 of Lectures in Applied Mathematics, American Math Society, 1990, pp. 100–118.

[4] T. SARPKAYA, *An inviscid model of two-dimensional vortex shedding for transient and asymptotically steady separated flow over an inclined plate*, J. Fluid Mech., 68 (1975), pp. 109–128.

[5] G. STRANG, *On the construction and comparison of difference schemes*, SIAM J. Num. Anal., 5 (1968), pp. 506–517.